



The New Storstrøm Bridge - Nonlinear Dynamic Ship Impacts

Martin N. Svendsen, Paola Bertolini, Frederik Vind

Ramboll

Contact: mnns@ramboll.com

Abstract

The New Storstrøm Bridge in Denmark is a 3800m long concrete girder bridge with 44 standard spans of mostly 80m and two navigational spans of 160m which are stay cable supported. The foundations are constructed as direct pad foundations, i.e. with the ability of the caissons to slide and rotate on gravel beds. The bridge supports two high-speed railway tracks and two lanes of road traffic. The waters of Storstrømmen are prone to high naval activity and this, in combination with relatively flexible foundations and high dynamic sensitivity of the girder due to train runability requirements, implies that ship impact scenarios are a critical design parameter. In the present paper, nonlinear dynamic ship impacts performed for the detail design are presented. The simulations include nonlinear representation of soil stiffnesses as well as ship indentation properties. Also, nonlinear geometric effects and strongly nonlinear bearing uplift effects are considered. Detailed descriptions of the complex structural response mechanisms occurring during critical ship impacts are provided and the influence of girder/pier tie-down cables on uplift magnitudes are presented.

Keywords: Structural dynamics; ship impact; computational design; bearing uplift, major bridges.

1 Introduction

The New Storstrøm Bridge in Denmark is a 3800m long concrete girder bridge with 44 standard spans of mostly 80m and two navigational spans of 160m which are stay cable supported. The foundations are constructed as direct foundations, i.e. with the ability of the caissons to slide and rotate on gravel beds. The bridge supports two high-speed railway tracks and two lanes of road traffic. Ramboll has been the main structural designer of the detailed design.

The waters of Storstrømmen are prone to high naval activity and this, in combination with relatively flexible foundations and high dynamic sensitivity of the girder due to train runability requirements, implies that ship impact scenarios are a critical design parameter. Also for the

Øresund Bridge and the Great Belt Bridge in Denmark, ship collision was found to be one of the most important load cases [1]. In the present paper the nonlinear dynamic ship impacts performed for the detail design are presented. The simulations include nonlinear representation of soil stiffnesses as well as ship deformation properties. Also, nonlinear geometric effects and as well as strongly nonlinear bearing uplift effects are considered.

The general arrangement of the bridge is shown in Figure 1. The bridge consists of three frames; the north frame, the central frame and the south frame. The longitudinal stability of the north and south frames is ensured by fixed piers at 14-12N and 13-15S respectively and by 1C for the central frame. All other piers and abutments have longitudinal sliding bearings. The three frames are connected by longitudinal shock transmission units

at the 6N/S expansion joints which seize for fast acting loads including dynamic wind, vertical traffic and braking. As such, the entire structure works as one combined system when resisting the most

critical loads. Tie-down cables are implemented at piers 1N and 1S and at the expansion joint piers at 6N and 6S. At the abutments, anti-uplift bearings are installed.

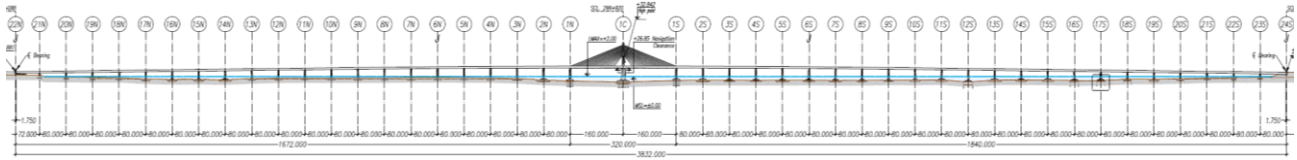


Figure 1. The New Storstrøm Bridge, general arrangement.

The global analysis has been performed using a single, coupled 3D beam element model to represent the entire system. The global model, see Figure 2, is 100% parametric, supporting rapid model updates and extensive use of computational design. This includes a full representation of all prestressing cables in girder and pylon as well as a sequential activation of these in a progressive construction stage analysis with detailed representation of creep, shrinkage and cable loss effects. The global model has been the basis of a highly automated structural design process, as presented in more detail in [3]-**Chyba! Nenalezen zdroj odkazů.**

Another important design consideration is associated with the shear keys. The capacity of these is governed directly by the ship impact load and similarly the tie-down cables are designed directly to limit bearing uplift to limit the required vertical working range of the shear keys. Finally, longitudinal pier top displacements are governing for the displacement capacity of the sliding bearings.

In the present paper two important impact scenarios are presented, namely an impact perpendicular to the bridge axis and a skew impact. This paper aims at providing an in-depth description of the complex structural response mechanisms occurring during ship impact, where the aforementioned nonlinearities are at play in the dynamic response.

The paper is organized as follows. Section 2 provides details of ship and bridge properties and in Section 3 the two reference ship impact cases are presented. In Section 4 the influence of different tie-down configurations on bearing uplift levels is presented. Sections 5 to 7 hold the conclusions, acknowledgements and references respectively.

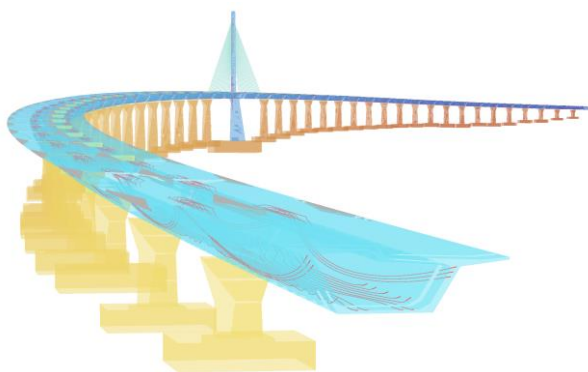


Figure 2. Global FE model.

The largest design ship loads occur for piers 2N to 2S near the navigational channel [2], and for the piers in this area the ship impact effects are governing the design of tie-down cables between girders and piers, shear keys between girders and piers, pier dimensions and caisson dimensions.

One important design criterion relates to global failure defined as a foundation displacement limit of 400mm due to ship impact which has been decisive in the design of some caissons.

2 Bridge and ship properties

In Figure 3 the girder, pier top and tie-down design at 1N/S is shown along with the functional layout of the bridge. The detail comprises two bearings and four tie-down cables. The shear key (not shown) is located at the vertical centerline. The asymmetrical layout in combination with the double curvature of the bridge alignment implies that the structural response even to simple static loads becomes non-trivial in terms of skew bending and torsion and requires a highly detailed model

representation to capture all relevant effects. Further, the girder width varies in the vicinity of the 1C pylon to accommodate the additional space needed for the stay cables and the pylon. The kink in the bridge deck is a result of geometric constraints including the height of the derailment barrier [4].

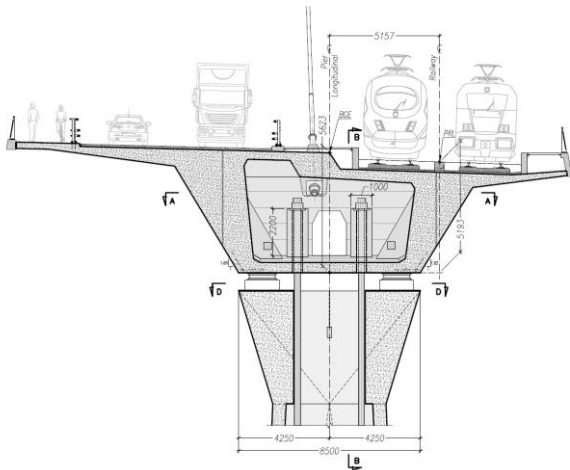


Figure 3. Girder and tie-down design at 1N/S.

Figure 4 shows the pier and caisson designs at 1S and 2S. Tie-down cables are only present at 1S. Further, inclusion piles are included at 1S while no soil strengthening is applied at 2S. It is noted that there is no structural connection between the caisson and the inclusion piles at 1S, i.e. the caisson is free to slide relative to the piles.

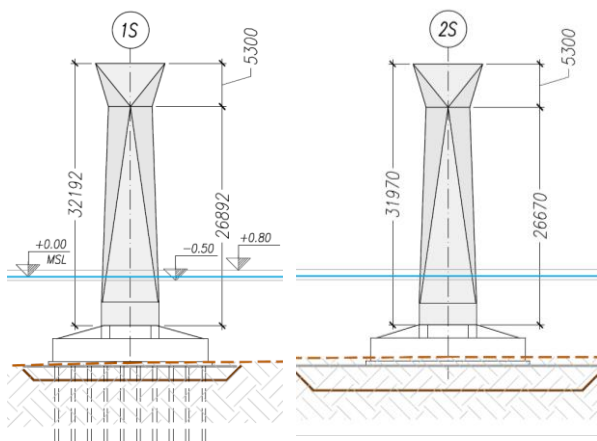


Figure 4. Pier and caisson geometries.

The design ships for the two cases considered here are defined as follows. The highest ship class for the present cases is a 6000 tonne DWT ship and in Figure 5 an example is shown. Ships of this type

have an average length of 108m (LPP) and an average breadth of 14.5m. For the perpendicular impact (Case 1), a low bow impact from a loaded 5000 tonne DWT vessel is applied.



Figure 5. Example of 6000 tonne DWT ship. [7]

This configuration generates the maximum transverse force in the foundation, at the lowest possible elevation, and this results in maximized foundation displacements. For the skew impact (Case 2), a higher bow/hull impact from a ballasted 6000 tonne DWT vessel is applied, and this high-elevation impact results in the largest rotations in the foundation, leading to maximized pier top displacements. The loaded and ballasted ships have maximum indentation forces of 65.5MN and 62.0MN, respectively, and the corresponding worklaws are shown in Figure 6. It is seen that the low bulb (Case 1) is assumed to have a lower stiffness than the higher bow/hull zone, but a higher maximum indentation force. No maximum indentation is defined in [2] and the shown end values are implementation limits which are not reached in the simulations.

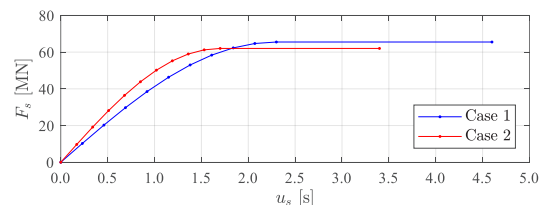


Figure 6. Ship indentation worklaws.

In Figure 7 the foundation worklaws at 1S are shown. It is noted that the maximum geotechnical capacity of appr. 50MN is significantly lower than the maximum impact force of 65MN. Although

some load sharing will take place with the superstructure for the transverse load component, this implies that the structural response can only be assessed by transient dynamic simulation where the limited duration of the impact is captured.

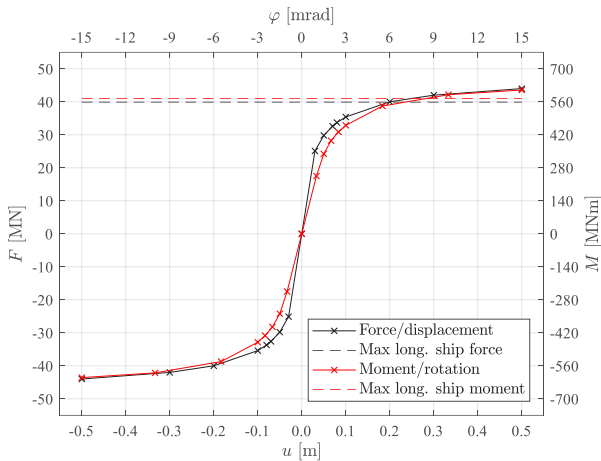


Figure 7. Foundation worklaws, 1S.

For the skew ship impact, a significant longitudinal load component must be absorbed by the pier itself. The maximum longitudinal force component and the associated moment at foundation level is plotted in Figure 7 and also in this case it is seen that due to the proximity of the load to the yielding plateau with the associated high sensitivity of the structural response to small load variations, accurate dynamic analyses are necessary. In the following section, details of the highly transient and nonlinear response mechanism due to the above properties are provided.

3 Reference ship impact cases

In the simulations, the ship is represented as a point mass with the ship impact velocity as initial condition. The mass is connected to the point of impact at the pier with a nonlinear spring representing the force/indentation worklaw of the ship.

In Figure 8 the force time histories of the ships F_s are shown along with corresponding ship velocities v_s . E.g. for Case 1 It is seen how the ship decelerates to a standstill at $t = 0.75s$, after which it accelerates in the opposite direction, partially due to accumulated elastic energy in the hull. At $t = 1.3s$ there is no longer contact between ship and pier and the ship drifts freely away from the bridge. The

exit speed is lower than the entry speed due to the energy dissipation in the nonlinear bow indentation spring as well as energy transfer to the bridge.

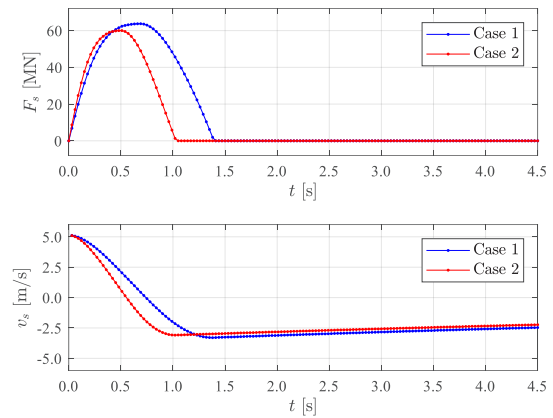


Figure 8. Ship forces and velocities.

In Figure 9 a structural deformation plot of the fully transverse impact (Case 1) is shown. The snapshot is taken at $t = 0.96s$ where the foundation displacement is largest.

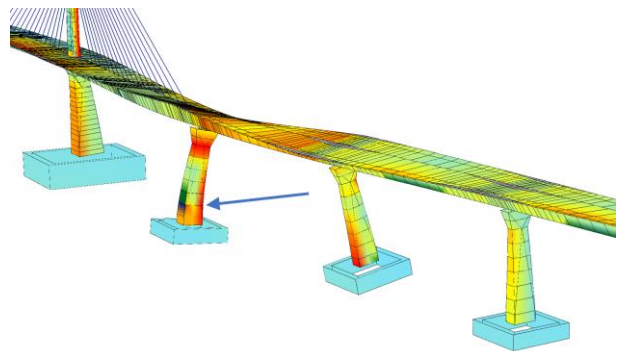


Figure 9. Case 1, $t = 0.96s$, deform. scale 1:70.

A similar deformation plot is shown for the skew impact (Case 2) in Figure 10.

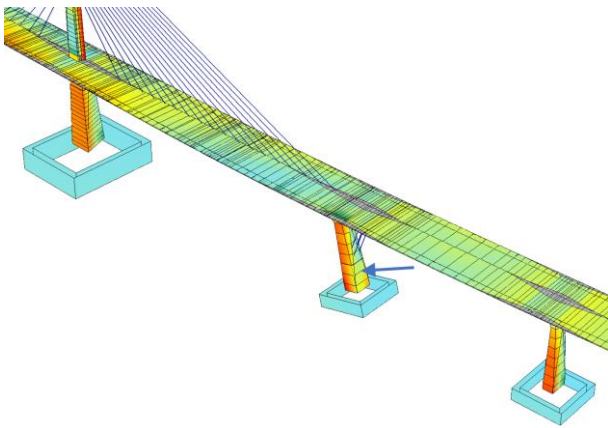


Figure 10. Case 2, $t = 0.99s$, deform. scale 1:20.

The snapshot is taken at $t = 0.99s$ where the longitudinal pier top displacement is the largest.

The corresponding foundation displacement responses perpendicular to the local bridge axis \bar{u}_y and parallel with the bridge axis \bar{u}_x for Case 1 and 2, respectively, are shown in Figure 11. It is seen that the peak displacements occur slightly after the maximum ship indentation forces occur. The delayed response represents a dynamic overshoot which increases with the mass of the foundation. However, also the soil stiffness increases with the mass of the foundation and in the present case the latter was found to be dominating.

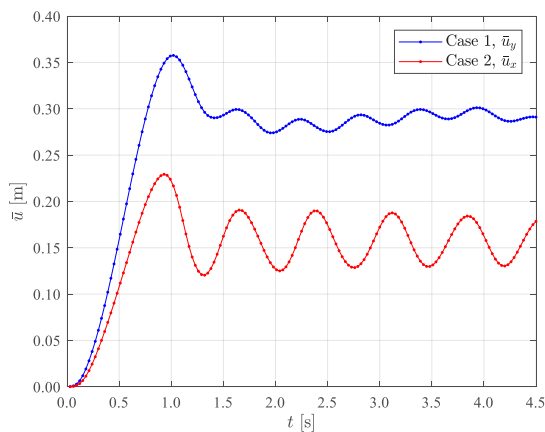


Figure 11. Foundation displacements, 1S.

Figure 12 shows the foundation displacement trajectories in global coordinates of the two cases along with the local bridge axis at the location of the pier and directions of impact.

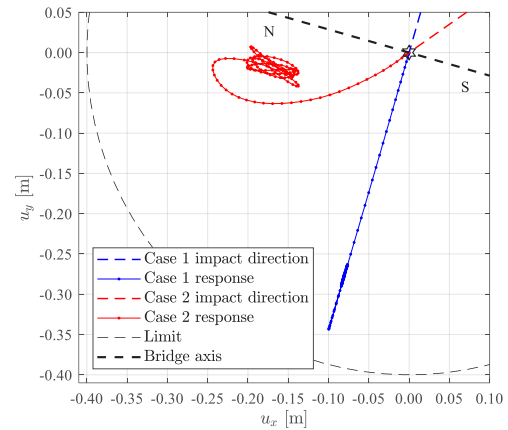


Figure 12. Foundation displacement trajectories.

For Case 2 the foundation is seen to initially follow the direction of the impact, and after some time it is diverted in the direction of the bridge axis. Towards the end of the response, the foundation is forced back towards the bridge axis by the girder. In both cases, the permanent deformation is within the depicted limit of 400mm.

In Figure 13 force/displacement trajectories are shown. It is seen that the responses are highly nonlinear, with significant plastic deformations. Due to the high utilization, the slightly larger load in Case 1 causes a much larger peak deformation.

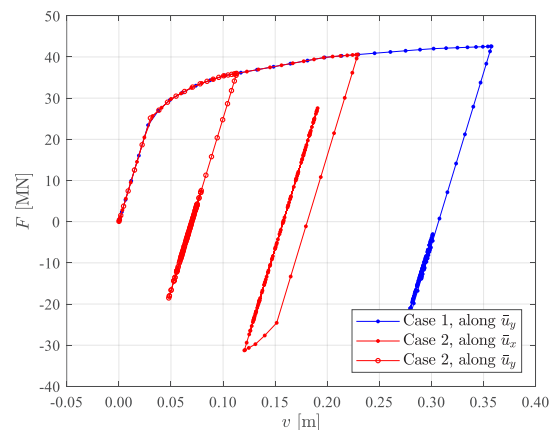


Figure 13. Displacements/forces, foundation 1S.

While the foundation displacement responses are qualitatively similar for the two cases, less similarity is observed for the rotational behavior, see Figure 14. Case 2 resembles a 1-dof-like behaviour also seen for the displacements, but for Case 1 the peak response is significantly delayed relative to the ship impact force.

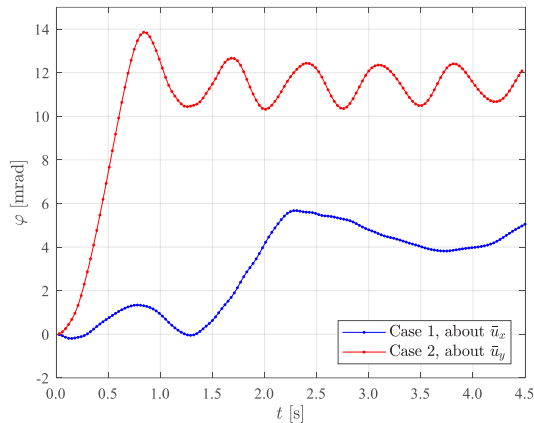


Figure 14. Rotation time histories, foundation 1S.

This mechanism is explained in the following. Initially, between 0.30s and 1.26s, a positive rotation occurs which corresponds to the deformations shown in Figure 9. The subsequent behaviour can be explained via Figure 15 showing pier top displacements. At $t = 0.96s$, the 1S pier top and girder is moving in the direction of the foundation which leads to the elimination of the foundation rotation at $t = 1.26s$.

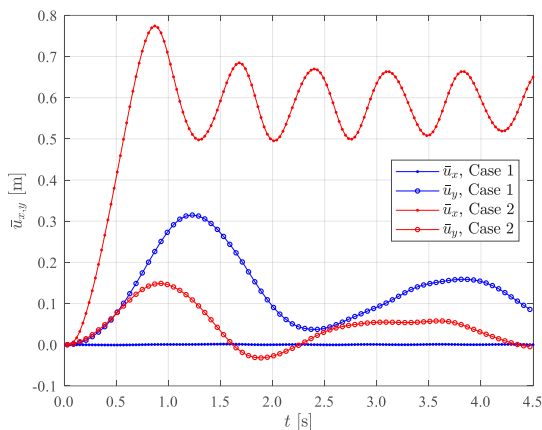


Figure 15. Top of pier displacements, 1S.

The deformations at $t = 1.26s$ are shown in Figure 16. In this state, pier 1S is largely undeformed while significant deformations are present in the girder and at pier 2S. The dynamic equilibrium at this point in time consists mainly of a balance between elastic and inertial forces in the girder where the girder velocity is momentarily close to zero.

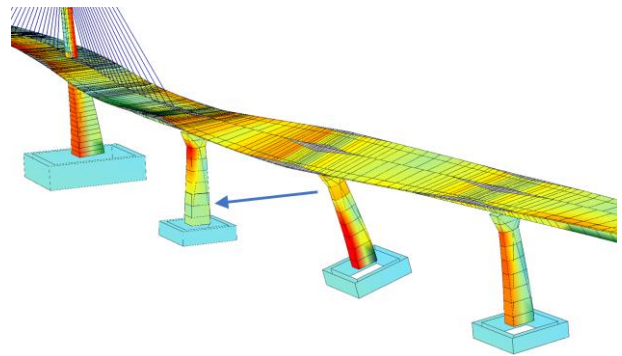


Figure 16. Case 1, $t = 1.26s$, deform. scale 1:70.

Subsequently, the girder returns towards its original location, resulting in the increase of the foundation rotation seen in Figure 14 between $t = 1.26s$ and $t = 2.34s$. In Figure 17 the deformations at $t = 2.34s$ are shown.

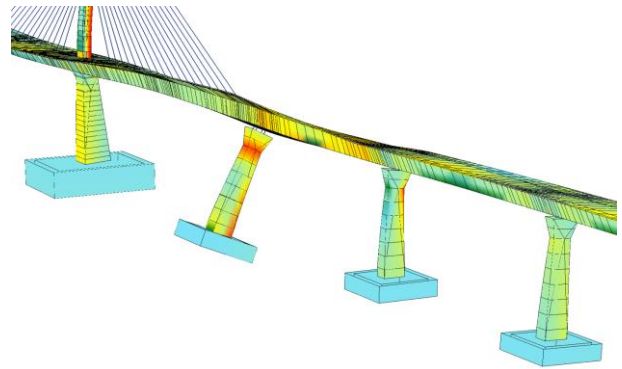


Figure 17. Case 1, $t = 2.34s$, deform. scale 1:70.

The initial rotation taking place in the time interval $t = 0.30s$ to $t = 1.26s$ is largely elastic and is seen in Figure 18 as a narrow trajectory on the elastic part of the force-displacement curve. The subsequent return of the girder generates a higher moment which activates the plastic behaviour of the foundation, leading to significantly larger rotations in the permanent state.

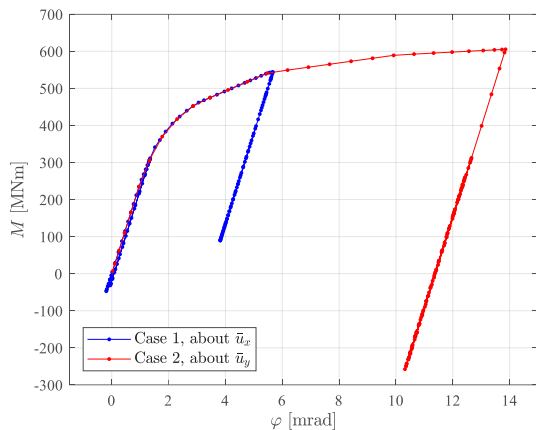


Figure 18. Rotations/moments, foundation 1S.

Impacts of the Case 2-type are decisive for the design of bearing sliding capacities due to the large pier top displacements that are generated. Impacts of the Case 1-type are decisive for the foundation footprint and ballast configuration. Increasing these properties leads to increased foundation stiffness and it is evident from the above plots that small design changes can lead to significant response changes.

Impacts of the Case 1-type are also decisive for the shear keys and tie-down cables. For the shear keys, one important effect is the shear force from the ship impact. Another important effect which is also critical for the tie-down cables, relates to the vertical working range of the shear keys. Considering again Figure 9, it is evident that the torsional stiffness of the girder combined with the foundation displacement at 1S will lead to compression reduction or potentially uplift at the eastern bearing of 1S and the western bearing of 2S. The shear keys are designed to have a vertical working range of 10mm, i.e. a maximum uplift in one bearing of 20mm can be accommodated when the other bearing at the same pier is closed.

In Figure 19, bearing forces F_B are shown for Case 1. It is seen that before the impact, the bearings are preloaded. In the present case a preloading corresponding to permanent effects alone, including stay stressing, tie-down stressing and creep and shrinkage effects is considered. It is seen how the initial compression at 1S East and 2S West is reduced due to the general deformation mechanism shown in Figure 9, and that in some periods the compressive forces are eliminated,

corresponding to bearing uplift. The uplift is a relatively strong nonlinearity which has set a lower limit for the simulation time step size.

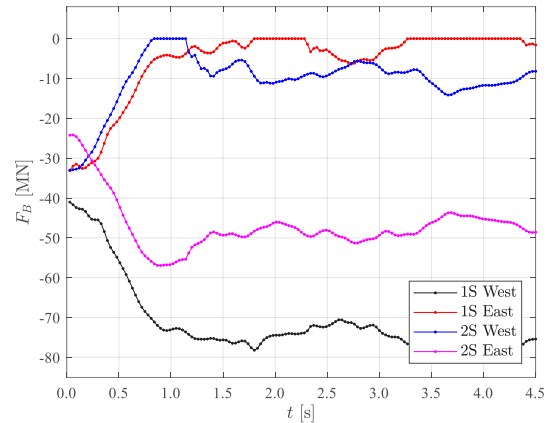


Figure 19. Bearing forces, Case 1.

The bearing openings u_B are shown in Figure 20. Similar to the foundation rotation, the critical opening of 1S East occurs relatively late at $t = 3.66s$, i.e. long after the ship impact has completed. This emphasizes how the complex transient dynamic response requires long simulations to capture all relevant effects. It is noted that considering nonlinear geometric effects, i.e. large displacements and rotations, is necessary to accurately determine the bearing openings, as they represent a significant nonlinear change of the structural geometry. This further implies that p-delta effects are inherently included in the results and that care must be taken to create accurate initial conditions for the simulation.

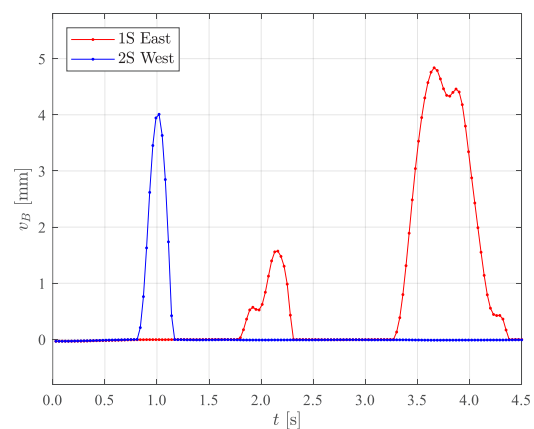


Figure 20. Bearing uplift, Case 1.

Several additional, more onerous, preload configurations in terms of e.g. different variable

load scenarios, have been investigated as part of the detailed design. In the following section, the specific effects of changing the tie-down cable configurations are presented in more detail.

4 Influence of tie-down cables

Given the bearing uplifts shown in Figure 20, several tie-downs solutions have been investigated to limit these effects in the most optimal way. Figure 21 shows how the maximum opening at 1S East can be almost linearly reduced by increasing the number of eastern tie-down cables n_{str} . The reference configuration is $n_{str} = 69$.

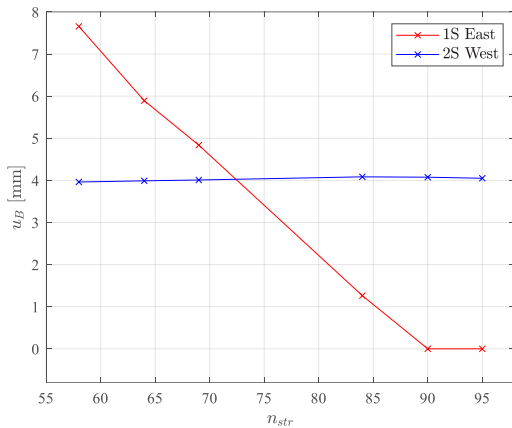


Figure 21. Maximum uplift vs. tie-down cables.

However, changing the tie-down configuration in pier 1S does not influence the uplift opening in the adjacent pier 2S bearings, as shown by the blue curve in Figure 21. This is due to the fact that the bearing uplift in pier 2S is mainly governed by transverse girder shear forces, which are not affected by the tie-down configuration.

As seen in Figure 9, significant out-of-plane bending M_z occurs in pier 1S during the impact. At the pier top, the associated moment is generated solely by the bearing forces, i.e. the local pier top girder diaphragm design becomes sensitive to the tie-down configuration. In Figure 22 the out-of-plane bending moment at the 1S pier top is shown for tie-down configurations with 58, 69, and 98 strands.

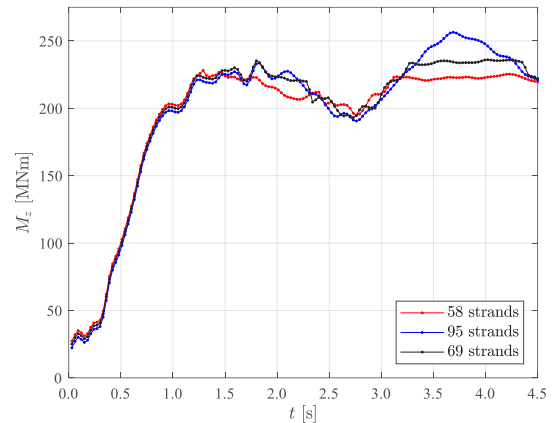


Figure 22. Pier top bending moment, 1S.

It is seen from Figure 22 that during the periods of uplift at 1S East, a smaller tie-down configuration leads to a smaller moment, because the connection between girder and pier is more flexible. As such, configuring the tie-down cables is a balance between on one hand limiting the maximum uplift to maintain the function of the shear key, and on the other hand limiting the compressive bearing loads, the local loads in the pier top and girder diaphragm and the use of cable steel.

5 Conclusions

In this paper, two important head-on bow ship impact scenarios are presented, namely an impact perpendicular to the bridge axis and a skew impact. In-depth descriptions of the complex structural response mechanisms occurring during ship impact have been provided. The importance of considering relatively long simulations, in the present case up to roughly three times the duration of the ship impact, has been demonstrated. This is important because of the critical effects are inertia-driven and occur long after the ship impact has completed. Further, the influence of different tie-down configurations on bearing uplift levels has been investigated, and an almost linear relation between the number of tie-down strands and the local maximum bearing uplift has been shown.

6 Acknowledgements

The Danish Road Directorate (DRD) and the Storstrøm Bridge Joint Venture (SBJV) are gratefully acknowledged for allowing publication of this paper. The initial design concept was



developed by Studio De Miranda Associati and the SBJV, based on the DRD's illustrative design.

7 References

- [1] L. Hauge, K. Olsen, O. Hededal, *Analysis of ship collision to pier and girder*, International Symposium of Advances in Ship Collision Analysis, May 10-13, Copenhagen, Denmark, 1998.
- [2] The Danish Road Directorate, *Design Basis of the New Storstrøm Bridge Rev. 3*, 2017.
- [3] Needham M., Collins J., *The New Storstrøm Bridge – Pier Design*, IABSE Symposium, Prague, Czech Republic, May 25-27, 2022.
- [4] Cagnino L., Po E., *The New Storstrøm Bridge – Prestressed Box Girder Design*, IABSE Symposium, Prague, Czech Republic, May 25-27, 2022.
- [5] Wharton J., Pedersen N. R., Bandeira F., Dimchev J., Särkkä E., Soppela S., *The New Storstrøm Bridge – Pylon and Stay Cable Design*, IABSE Symposium, Prague, Czech Republic, May 25-27, 2022.
- [6] MacAulay B., Larsen E. S., *New Cable Stayed Bridge Across Storstrømmen*, 40th IABSE Symposium, Nantes, France, September 19-21, 2018.
- [7] [Vesselfinder.com](https://www.vesselfinder.com)